Quantum dynamics of radiationless electronic transitions including normal modes displacements and duschinsky rotations: A second-order cumulant approach

Borrelli, Raffaele; Peluso, Andrea. Quantum dynamics of radiationless electronic transitions including normal modes displacements and duschinsky rotations: A second-order cumulant approach. JOURNAL OF CHEMICAL THEORY AND COMPUTATION. 11 (2) pp: 415-422.
DOI: 10.1021/ct500966c

Quantum dynamics of radiationless electronic transitions including normal modes displacements and Duschinsky rotations: a second-order cumulant approach

Raffaele Borrelli[*,†] and Andrea Peluso[‡]

Department of Agricultural, Forestry and Food Science, University of Torino, I-10195 Grugliasco, Italy, and Department of Chemistry and Biology, University of Salerno, I-84081 Fisciano, Italy

E-mail: raffaele.borrelli@unito.it

Abstract

An analytical expression for the population dynamics of electronic radiationless transitions has been derived from the second order expansion of the quantum evolution operator in the Liouville space and the cumulant theory. The expression includes the effect of both normal mode displacements and Duschinsky rotations and allows to take into account both equilibrium and non-equilibrium initial conditions. The methodology has been applied to model the electron-transfer process between the accessory bacteriochlorophyll and the bacteriopheophytine in bacterial reactions centers, providing a rate in good agreement with experimental findings.

[*]To whom correspondence should be addressed
[†]Department of Agricultural, Forestry and Food Science, University of Torino, I-10195 Grugliasco, Italy
[‡]Department of Chemistry and Biology, University of Salerno, I-84081 Fisciano, Italy

1 Introduction

The widespread applications of time-resolved spectroscopy to molecular processes together with the need of understanding the mechanism of complex light driven biochemical systems at microscopic level have thrown new challenges to the theory of time-dependent molecular processes.[1,2] Nowadays electronic wave function calculations provide impressively accurate information about the potential energy surfaces (PES) of large molecular systems both for ground and excited states. Combining such precious information with quantum dynamics simulations could hopefully open new routes for improving our knowledge on radiationless transitions, which control many biochemical and technological processes. Although powerful methodologies capable of handling molecular systems with a large number of degrees of freedom and complex molecular Hamiltonians have been developed[3–6] their use, is often limited by their algorithmic complexity and high computational costs. There are two possible ways out: i) to employ model Hamiltonians with a small number of 'active' nuclear degrees of freedom, i.e. modes whose quantum state can change upon transition, and solving numerically the associated time-dependent Schrödinger equation; ii) to resort to time-dependent perturbation theory for approximate solutions of the Schrödinger equation, retaining the whole space of coordinates or momenta.[7–12]

Obviously, the choice between the two alternative approaches should be based on a careful analysis of the potential energies of the two electronic states involved in the transition. Approach i) should be preferred when the high symmetry of the system poses limits to the number of the active modes, as in the case of $S_2(B_{2u}) \rightarrow S_1(B_{3u})$ transition of pyrazine.[13,14] In all other cases, namely in the presence of significantly large nuclear displacements and high reorganization energies, the selection of a reduced space of active nuclear coordinates can be very difficult and arbitrary. Indeed, even for the case of relatively small molecules such as guanine and adenine, the analysis of the PESs reveals that the number of nuclear degrees of freedom displaced or rotated upon hole transfer is large enough to prevent a simple numerical solution of the time-dependent Schrödinger equation.[15] In those cases, the Fermi

Golden Rule (FGR) has been widely used, despite its intrinsic limitations, due to the fact that it is based on the lowest orders of time-dependent perturbation theory, in which the upper limit of time integration is set to infinity. Indeed, in most chemico-physical processes the population decay of an initial state or the build up of the populations of transient and final states are often well represented by a single exponential function and therefore an estimate of the quantum dynamical behaviour of the system in terms of a global reaction rate is well sound.

A significant improvement with respect to FGR can be obtained using a second-order cumulant expansion of the reduced density matrix of the system. The cumulant approach,[16–22] recently discussed and successfully applied to spin-boson and linear vibronic coupling Hamiltonian model,[23–26] allows to take into account the change of the reaction rate with time, describing the population $P(t)$ of the state of interest with an equation of the form

$$\frac{dP(t)}{dt} = k(t)P(t). \tag{1}$$

In this paper we extend this approach to treat the general case of transitions involving changes in the nuclear equilibrium positions as well as higher order effects such as Duschinsky normal modes rotations and frequency changes, handling the case of initial states prepared both in a thermally equilibrated population and in a generic non-equilibrium initial distribution, as it occurs in ultrafast processes initiated by a short laser pulse.[27,28] The methodology is then applied to the case of fast electron transfer between the accessory bacteriochlorophyll and the pheophytine in bacterial reactions centers and compare the results with those obtained using the standard Golden Rule approach.

2 Theory

The model Hamiltonian used throughout this paper includes two electronic states, $|A\rangle$ and $|F\rangle$, coupled each other through a generic operator V_{AF}

$$H = |A\rangle H_A \langle A| + |F\rangle H_F \langle F| + V_{AF} |A\rangle \langle F| + \text{c.c.} = H_0 + V \tag{2}$$

where $H_{A,F}$ are the vibrational Hamiltonian of the electronic states $|A\rangle$ and $|F\rangle$ respectively. The definitions of H_0 and V follow immediately.

For H_A and H_F we assume that harmonic approximation holds, retaining two different sets of normal coordinates for each electronic state:

$$H_A = \sum_i^N \omega_{Ai}/2(p_{Ai}^2 + q_{Ai}^2) + E_A^\circ \tag{3}$$

$$H_F = \sum_i^N \omega_{Fi}/2(p_{Fi}^2 + q_{Fi}^2) + E_F^\circ \tag{4}$$

The two sets of dimesionless normal coordinates are related by the affine transformation:

$$q_F = d_F + J_F q_A \tag{5}$$

where J_F is the normal mode transformation matrix and d_F the displacement vector.[29–31] Dimensionless coordinates are defined, as usual, in terms of standard normal coordinates (Q) as

$$q_X = \gamma_X^{1/2} Q_X \qquad \gamma_X = 2\pi c \omega_X/\hbar \qquad X = A, F.$$

The nuclear vibrational Hamiltonian considered in this work is the most general model of an ensemble of harmonic oscillators. Upon the electronic transition the oscillators are allowed to change not only their equilibrium position, but also their frequency and their direction. Nowadays, the parameters necessary to model H_A and H_F can be reliably obtained from

electronic structure calculations, at least for medium sized and non floppy molecules.[32–34] Second-order effects such as variations of vibrational frequencies and the directions of normal vibrations, are usually not included in most of the Hamiltonian models used in qunatum dynamics, though a number of works suggest that their effect can be quite relevant.[35–40]

The coupling operator V_{AF} is in general a function of the vibrational coordinates of the system, although it is quite common to assume its value constant, since electronic transitions take place in a restricted region of the nuclear coordinates.[41] Another approximation of V_{AF}, widely used in the study of photoexcited decays where conical intersections play a major role, is the so called linear vibronic model[1,42,43] in which the coupling operator is a linear function of the nuclear coordinates. In this paper we will develop a formalism which can handle both cases.

The equation governing the evolution of the density matrix in the interaction representation $\rho_I(t)$ is formally given by

$$\rho_I(t) = \mathcal{T} e^{-i\int_0^t V_I^{\times}(\tau)d\tau/\hbar}\rho_I(0)$$

where $\mathcal{T}$ is a properly chosen time ordering operator, and $\rho_I(0)$ is the density at $t = 0$. The operator $V_I^{\times}(\tau)$ is defined, as usual, by its action on a generic operator O as $V_I^{\times}(\tau)O = [V_I(\tau), O]$.[18,44] This is only a formal solution since its evaluation requires the expansion of the exponential and the application of the $\mathcal{T}$ operator.

The population of the initial electronic state $|A\rangle$ is formally given by

$$P_A(t) = \mathrm{Tr}\big\langle A\big|\mathcal{T} e^{-i\int_0^t V_I^{\times}(\tau)d\tau/\hbar}\rho_I(0)\big|A\big\rangle = \left\langle \mathcal{T} e^{-i\int_0^t V_I^{\times}(\tau)d\tau/\hbar}\right\rangle$$

where, $\langle X\rangle = \mathrm{Tr}\{\langle A|\, X\rho_I(0)\,|A\rangle\}$, and the trace is taken over the vibrational degrees of freedom. From the formally exact expression above we use the cumulant expansion and

truncate it to second order following the general theory developed by Kubo[18,19]

$$P_A(t) = \left\langle \mathcal{T} e^{-i\int_0^t V_I^{\times}(\tau)d\tau/\hbar} \right\rangle = \exp K(t) \tag{6}$$

where

$$K(t) = \sum_n^{\infty} K_n(t) = \sum_{n=1}^{\infty} \frac{1}{n!}\left(\frac{-i}{\hbar}\right)^n \int_0^t d\tau_1 \cdots \int_0^t d\tau_n \left\langle \mathcal{T} V_I^{\times}(\tau_1)...V_I^{\times}(\tau_n)\right\rangle_c$$

and $\langle ... \rangle_c$ is the so-called cumulant average.

It is immediate to show that in our model the first order cumulant $K_1(t)$ is zero, thus the second order approximation becomes

$$P_A(t) = \exp(K_2(t)) = \exp\left(-\hbar^{-2}/2 \int_0^t \int_0^t \left\langle \mathcal{T} V_I^{\times}(\tau_1) V_I^{\times}(\tau_2)\right\rangle_c d\tau_1 d\tau_2\right). \tag{7}$$

Using the standard definition of the time ordering operator the second order cumulant $K_2(t)$ can be rewritten as

$$K_2(t) = -\hbar^{-2} 2\mathrm{Re} \int_0^t \int_0^{\tau_1} \left\langle A\right| [V_I(\tau_2), [V_I(\tau_2), \rho_\circ]] \left|A\right\rangle d\tau_1 d\tau_2. \tag{8}$$

The final form of $K_2(t)$ depends on the explicit expression of the initial density of the system, $\rho_\circ$. In ground state processes this is usually assumed to be the equilbrium population of the unperturbed initial state $|A\rangle$, while in excited state decay processes the system is usually prepared in a non-equilibrium condition. Indeed, in the general picture of a photophysical process a molecular system is initially found in its unperturbed and thermally equilibrated ground electronic state, $|G\rangle$, which is instantaneously excited by a pump pulse into an electronic excited state $|A\rangle$. The resulting excited state density is just the Boltzmann equilibrium distribution of state $|G\rangle$ projected onto the photoexcited state $|A\rangle$

$$\rho_\circ = Z_G^{-1} \left|A\right\rangle e^{-\beta H_G} \left\langle A\right|.$$

where Z_G is the ground state vibrational partition function. Using this initial density and eq 8 the second order cumulant becomes

$$K_2(t) = -\hbar^{-2} Z_G^{-1} \mathrm{Re} \int_0^t \int_0^t \mathrm{Tr}(e^{-\beta H_G} e^{iH_A^\circ \tau_2} V_{AF} e^{-iH_F(\tau_2-\tau_1)} V_{FA} e^{-iH_A\tau_1}) d\tau_1 d\tau_2. \quad (9)$$

Thus, the evaluation of the double integral of equation 9 allows, in principle, to calculate the population of the system at any given time t.

A better insight into the above equation can be obtained by writing the differential equation governing the electronic population (obtained by simply differentiating eq. 7 with respect to t)

$$\frac{dP_A(t)}{dt} = k(t) P_A(t) \quad (10)$$

where

$$k(t) = -2\hbar^{-2} Z_G^{-1} \mathrm{Re} \int_0^t \mathrm{Tr}(e^{-\beta H_G} e^{itH_A} e^{-i\tau H_F} e^{-i(t-\tau)H_A}) d\tau \quad (11)$$

can be interpreted as a time-dependent rate of the electronic transition. If we assume that the correlation time τ_c of $V_I^\times(\tau)$ is much smaller than a characteristic transition time of the system then we can let t to infinity and define a non-equilibrium rate constant, k_{NGR}, as $k_{\mathrm{NGR}} = k(\infty)$.[24]

In case the initial density coincides with the thermal distribution of the state $|A\rangle$ the result discussed above can be simplified as

$$k(t) = -2\hbar^{-2} Z_G^{-1} \mathrm{Re} \int_0^t \mathrm{Tr}(e^{iH_A(\tau+i\beta)} V_{AF} e^{-iH_F\tau} V_{FA}) d\tau \quad (12)$$

and the solution of equation 10 can be written as

$$P_A(t) = \exp\left(\int_0^t k(s)(t-s) ds \right). \quad (13)$$

A major result of this work is the derivation of a closed expression for the time-dependent

rate $k(t)$ in terms of quantities easily obtainable from electronic structure calculations. Moreover, this epression is particularly suitable for numerical computations. Indeed, as shown in the appendix, the evaluation of the traces over the vibrational degrees of freedom in eq.s 11 and 12 can be handled using the theory of density matrices of multidimensional harmonic oscillators.[9,45] In the case of a constant coupling operator, $V_{AF} = V$, equation 12 becomes

$$k(t) = -2\hbar^{-2}V^2 \mathrm{Re} \int_0^t f_\circ(\tau) d\tau \tag{14}$$

with the correlation function $f_\circ(\tau)$ defined as

$$f_\circ(\tau) = Z_G^{-1}\mathrm{Tr}(e^{iH_A(\tau+i\beta)}e^{-iH_F\tau}) = Z_G^{-1}\Phi(\tau)\det(A(\tau))^{-1/2}\exp\Big[\frac{1}{2}\tilde{B}(\tau)A^{-1}(\tau)B(\tau)\Big] \tag{15}$$

where the definitions of A, B and Φ are given in the appendix. An analogous expression can be derived for equation 11.

The formulation discussed above can be easily extended to treat cases in which the coupling operator is a function of the nuclear coordinates, providing a tool to describe the dynamics close to a conical intersection.[1] Indeed, it can be shown that if $V_{AF} = \lambda q_i$, where λ is a real constant, the correlation function is given by

$$f(\tau) = f_\circ(\tau)\left[\frac{(A^{-1})_{ij}}{2} + \sum_j (A^{-1})_{ij}B_j\right]. \tag{16}$$

with $j = i + N$, N being the number of vibrational degrees of freedom. The derivation of the above expression is given in the appendix.

Finally, it should be noted that the same technique can also be used in the momentum representation, thus allowing to treat cases in which the coupling operator V_{AF} is the so-called non-adiabatic derivative coupling ($V \propto \frac{\partial}{\partial q_i}$). Indeed it should be recalled that the density matrix of an ensemble of harmonic oscillators has the same exact functional form both in the coordinate and in the momentum representation.

3 Fast electron-transfer in photosynthetic reactions centers

The methodology described above has been applied to the analysis of ultrafast electron-transfer (ET) between the accessory bacteriochlorophyll (B_A) and the bacteriopheophytin (H_A) in bacterial reactions centers.

In a previous paper we have already analyzed the dynamics of the ET process solving numerically the time-dependent Schrödinger equation in a reduced space of nuclear coordinates.[46] Only 16 vibrational modes, among more than 50 displaced modes yielded by DFT computations, were considered in dynamics. Here we will tackle the same problem, taking into consideration the whole set of normal coordinates, by means of both the FGR in its standard formulation and the second-order cumulant approach.

Following our previous work, the "diabatic" electronic states have been taken as the direct product of the neutral and anionic states of the two single molecules, *i.e.* $|A\rangle = \left|B_A^-\right\rangle |H_A\rangle$ and $|F\rangle = |B_A\rangle \left|H_A^-\right\rangle$. Equilibrium geometries, normal modes, and vibrational frequencies of bacteriochlorophyll and bacteriopheophytin in their neutral and anionic forms were obtained at the DFT level using the standard B3LYP functional with a 6-311+G(d,p) basis set. In order to obtain reliable estimates of the molecular parameters which characterize H_A and H_F, we have preferred to compute them for the isolated redox cofactors in the gas phase by using the highest level of computation compatible with the size of the molecules.[47] The Duschinsky transformation has been computed using the internal coordinate representation of normal modes.[33,48–50] The use of curvilinear internal coordinates is of crucial importance to avoid the appearance of fictious vibrational progressions in the computed density of states.[48,51,52] In the present case the reorganization energies of B_A/B_A^- and H_A/H_A^- pairs computed using Cartesian coordinates and harmonic approximation are 3396 cm^{-1} and 1454 cm^{-1} , respectively, while those obtained using internal coordinates are 925 cm^{-1} and 993 cm^{-1} , respectively. For B_A/B_A^- the reorganization energy obtained from Cartesian coordinates is

almost four times larger than that computed using internal coordinates. Since the electronic dynamics is strongly dependent on these parameters the use of internal coordinates is highly recommended for future applications.

With the adopted choice of diabatic states, the computation of the trace of Eq. 11 can be factorized into the product of two correlation functions associated with the electron detachment from B_A^- and the electron attachment to H_A, thus halving the computational cost.

All the other parameters necessary for defining the Hamiltonian of Eq. 2 have been taken from Ref. 46: V_{AF} is set to 90 cm^{-1} while ΔE_{AF} is allowed to vary in the range 1250–1450 cm^{-1} .

Figure 1 shows the computed Franck-Condon (FC) spectra, at T=298 K, for the electron detachment from B_A^- and for the electron attachment to H_A. Both spectra are quite narrow, extending over a region of about 5000 cm^{-1} . The band around 1700–2000 cm^{-1} arises mainly from the excitation of three vibrations of B_A falling at $1648, 1731, 1764$ cm^{-1} and of the vibration of H_A^- at 1703 cm^{-1} . The latter involving the stretching vibration of the carbonyl group, one among the most displaced modes upon ET for both molecules.

Figure 2 shows the FC weighted density of states (FCWD) for the overall electron-transfer process from B_A^- to H_A, obtained from the convolution of the two normalized spectra. As usual, for any transition between two electronic states $|A\rangle$ and $|F\rangle$, this quantity is defined as

$$\mathrm{FCWD(E,T)} = \sum_{n,m} p_{Am}(T)|\langle m|n\rangle|^2 \delta(E_{Fn} - E_{Am} - E)$$

where E_{Fn}, E_{Am} are the energies of the vibrational eigenstates $|n\rangle$, $|m\rangle$ of the two electronic states, $p_{Am}(T)$ is the population of the initial states, and $|\langle m|n\rangle|^2$ is the FC factor. Assuming that the electronic coupling between the two electronic state is independent of coordinates, we obtain from the FC weighted density of states the FGR rate of ET as a function of ΔE_{AF}:

$$k(\Delta E, T) = \frac{2\pi}{\hbar}|V_{AF}|^2 \mathrm{FCWD}(\Delta E, T).$$

At T=298 K and for $\Delta E = 1350$ cm^{-1} the kinetic constant for the decay of $|A\rangle$ is 2.25 ps^{-1}, a value which compare reasonably well with the available experimental results. Indeed, it is not an easy task to assign a transition time to ET from B_A^- to H_A. The involvement of the monomer bacteriochlorophyll B_A as an intermediate electron acceptor, leading to the formation of the charge-separated state $P^+B_A^-$, has been debated for a long time in the literature, probably because the characteristic absorption region for the monomer bacteriochlorophyll, around 800 nm, is highly congested. The excited state of the special pair of chlorophylls (P^*) has a lifetime of ca. 3 ps; within this time interval, spectral features attributable to the formation of the bacteriopheophytin anion (H_A^-) can be identified. Early time-resolved pump-probe measurements, probing the region of the bleaching of the ground-state absorption of P (870 nm) and that of H_A (545 nm) and the appearance of the bacteriopheophytin anion (660 nm), gave no indication of the involvement of an intermediate electron acceptor.[53] It was concluded that the presence of B_A served to facilitate the direct electron transfer between P^* and H_A via a super-exchange ET mechanism. Subsequent measurements, probing the spectral region in which the anion of the monomer bacteriochlorophyll is expected to absorb (1020 nm), gave an indication for the formation of the charge-separated state $P^+B_A^-$, which occurs with a time constant of ca. 1 ps.[54,55]

Figure 3a shows the overall population decay of the state $\left|B_A^- H_A\right\rangle$ at 298 K as a function of time, obtained by the second order cumulant approximation when the system is initially found in an equilibrium condition. The curves correspond to different values of the energy difference between the initial and final states (see figure caption for details). In all cases the long-time behaviour of the curves is clearly exponential, as it can be better appreciated from inspection of figure 3b where the rate constant $k(t)$ is reported as a function of the time. For all ΔE_{FA} considered, the time-dependent rate exhibits a very fast decay followed by smooth oscillations, rapidly (within 50 fs) reaching a limiting value, which corresponds exactly to that obtained by the standard Fermi Golden Rule using the weighted density of states of figure 2.

Figure 3c shows the difference between the population of the initial state as obtained from the exact second order expression and the exponential decay of the standard FGR approach, *i.e.*$\Delta P(t) = \exp(\int_0^t k(s)ds - k_{\mathrm{FGR}}t)$. For short times the population dynamics deviates from the single exponential decay model, though, in the present case, the difference is not very large, being at most 0.02 at 500 fs.

Figure 4a and 4b shows the overall population decay of the state $\left|B_A^- H_A\right\rangle$ as a function of time and the time-dependent rate $k(t)$, respectively, when the system is initially found in a non-equilibrium distribution. The non-equilibrium distribution is obtained assuming that the electron is suddenly injected into B_A and the anion state has not enough time to relax to its a thermal equilibrium distribution. As in the previous case the rate constant shows a series of oscillations for short times, though less pronounced, and rapidly approaches a limiting value. For short times the non-equilibrium and the equilibrium rates show significant differences, while their limiting values are quite similar. In the energy range examined here, the rate increases as the energy difference between the initial and final states increases, and in all cases the NGR limiting values are slightly smaller than the equilibrium ones. Figure 4a shows the difference between the electronic populations obtained from the second order expression and the exponential decay obtained from the asymptotic value of the non-equilibrium rate $k_{\mathrm{NGR}}(\infty)$. The difference is less pronounced than in the equilibrium case, in agreement with the tendency of $k(t)$ to reach its asymptotic value in a shorter time and with smaller oscillations.

It is hard to disentangle the factors which are at the origin of the two different behaviours of $k(t)$. In the case of a non-equilibrium process the system is initially prepared in a state that is not an eigenstate of the zero-th order Hamiltonian. The initial state can undergo a fast dephasing process, whose overall effect is to quickly damp the oscillations of the time-dependent rate attaining its asymptotic value in a very short time. This effect could be less pronounced when the system is initially found in an eigenstate of the zero-th order Hamiltonian as in the standard FGR treatment.

4 Discussion

The second-order cumulant approximation of the electronic population dynamics derived in this paper provides an affordable methodology for the study of electronic transitions in large molecular systems. The methodology, though approximate, employs a fully quadratic Hamiltonian and includes two fundamental physical effects that influence the overall dynamics, *i.e.* the displacement of equilibrium position and the change of vibrational frequency and direction of the normal vibrations (Duschinsky effect). The method developed in this work can be applied to any transition operator having the form of a power series either of the vibrational coordinates, or of the vibrational momenta. It is thus of interest for the analysis of the dynamics of electron-transfer reactions as well as of ultrafast radiationless transitions induced by conical intersections. To our knowledge, this is the first implementation of the second-order cumulant expression using this type of Hamiltonian operator. Finally, it provides an improvement over the standard FGR treatment, and allows to asses whether a simple kinetic approach can be adopted for the process under examination.

The method has been applied to the study of the sub-picosecond electron-transfer reaction between the accessory bacteriochlorophyll and the bacteriopheophytin in bacterial reaction centers. The computed time-dependent rates $k(t)$ show an ultrafast decay followed by a series of damped oscillations and attain rapidly their limiting value. This result shows that, in this specific application the FGR approximation is well sound.

The computed transition rate at room temperature, obtained by a least-square fitting of the computed decay curve is about 2.2 ps^{-1}, in good agreement with the observed kinetic data which set the transition rate around 1.1 ps^{-1}. Due to the qualitative estimate of the coupling parameter adopted in this paper, this error seems most justifiable. The above results clearly show that the methodology is well suited to describe sub-picoseconds processes taking into account non-equilibrium initial condition, which, as discussed by Parson and Warshel[27,56] are important to properly describe photoindiced ET processes.

Finally, we note that the mathematical description of the correlation functions developed

in this paper is well suited for extending the theory to higher order terms of the cumulant expansion. Work is in progress along this direction.

5 Appendix A

The evaluation of the time-dependent rates $k(t)$ of equations 11 and 12 is based on the coordinate representation of the density matrices followed by the analytical evaluation of multidimensional Gaussian type integrals. We consider first the case in which the initial density matrix is represented by a thermally equilibrated state, and the coupling operator is a constant factor $V_{AF} = V$. In this case the time-dependent rate is written as

$$k(t) = -2V^2\hbar^{-2}Z_G^{-1}\mathrm{Re}\int_0^t \mathrm{Tr}(e^{iH_A(\tau+i\beta)}e^{-iH_F\tau})d\tau. \tag{17}$$

The trace can be evaluated in the coordinate representation as

$$f_\circ(\tau) = Z_G^{-1}\mathrm{Tr}(e^{iH_A(\tau+i\beta)}e^{-iH_F\tau}) = Z_G^{-1}\int dq_A \left\langle q_A\right| e^{-(\beta-i\tau)H_A}e^{-i\tau H_F}\left|q_A\right\rangle = Z_G^{-1}\int dq_A dx_A \rho_A(q_A, x_A, \beta - i\tau)\rho_F(x_A, q_A, i\tau). \tag{18}$$

Here the variables x_A, q_A represents two sets of normal coordinates of the state $|A\rangle$. The integration is carried on in the space of the normal coordinates of state A. If q_F represent the normal coordinates of state $|F\rangle$ then $q_F = d_F + J_F q_A$ where d_F is the vector of dimensionless displacements of normal coordinates and J_F the Duschinsky matrix, the density matrix ρ_F becomes

$$\rho_F(x_A, y_A, \lambda) = |\det(J_F)|[\det(2\pi\sinh(\lambda\omega_A))]^{-1/2}$$
$$\exp\Big\{-1/4(x_A + y_A + 2\Delta_F)\tilde{J}T_F(\lambda)J(x_A + y_A + 2\Delta_F) - 1/4(x_A - y_A)\tilde{J}C_F(\lambda)J(x_A - y_A)\Big\}$$

where

$$\Delta_F = J_F^{-1} d_F; \qquad T_F(\lambda) = \tanh(\lambda\omega_F/2); \qquad C_F(\lambda) = \coth(\lambda\omega_F/2).$$

Equation 18 can thus be written as

$$f_\circ(\tau) = Z_G^{-1}(2\pi)^{-N} |\det(J_F)| \exp(-\tilde{d}_F T_F d_F) D_A(\beta - i\tau) D_F(i\tau) \int du \exp\left(-\frac{1}{2}\tilde{u}Au + Bu\right) \tag{19}$$

where

$$A(\tau) = \frac{1}{2}\begin{pmatrix} M_A(\beta - i\tau) + M'_F(i\tau) & S_A(\beta - i\tau) + S'_F(i\tau) \\ \tilde{S}_A(\beta - i\tau) + \tilde{S}'_F(i\tau) & M_A(\beta - i\tau) + M'_F(i\tau) \end{pmatrix}$$

$$\tilde{B}(\tau) = -\begin{pmatrix} \tilde{J}_F T_F(i\tau) J_F \Delta_F \\ \tilde{J}_F T_F(i\tau) J_F \Delta_F \end{pmatrix}.$$

and the functions $D_X(\lambda)$, $M_X(\lambda), S_X(\lambda)$ and $M'_X(\lambda), S'_X(\lambda)$, $(X = A, F)$ are defined as

$$D_X(\lambda) = [\det(\sinh(\lambda\omega_X))]^{-1/2}$$

$$M_X(\lambda) = T_X(\lambda) + C_X(\lambda); \qquad S_X(\lambda) = T_X(\lambda) - C_X(\lambda)$$

$$M'_X(\lambda) = \tilde{J} M_X(\lambda) J; \qquad S'_X(\lambda) = \tilde{J} S_X(\lambda) J.$$

Using standard methods for evaluation of Gaussian integrals we have

$$f_\circ(\tau) = \Phi(\tau) \det[A(\tau)]^{-1/2} \exp\Big[\frac{1}{2}\tilde{B}(\tau) A^{-1}(\tau) B(\tau)\Big] \tag{20}$$

with

$$\Phi(\tau) = Z_G^{-1} |\det(J_F)| \exp(-\tilde{d}_F T_F d_F) \left[\det(\sinh((\beta - i\tau)\omega_A)) \det(\sinh(i\tau\omega_F))\right]^{-1/2}.$$

It is also worth mentioning that the functions $M_X(\lambda), S_X(\lambda)$ can be written in a more

compact form as

$$M_X(\lambda) = 2[\tanh(\lambda\omega_X)]^{-1}; \qquad S_X(\lambda) = -2[\sinh(\lambda\omega_X)]^{-1},$$

and, in the case of a purely imaginary $\lambda = i\tau$, we have

$$M_X(i\tau) = -2i[\tan(\tau\omega_X)]^{-1}; \qquad S_X(i\tau) = 2i[\sin(\tau\omega_X)]^{-1}.$$

This formalism allows to easily extend the treatment to cases in which the coupling V_{AF} is a function of nuclear coordinates or momenta. Indeed, if $V_{AF} = \lambda q_i$, where λ is a real constant, the correlation fuction of the form

$$f(\tau) = \lambda^2 \mathrm{Tr}(q_i e^{iH_A(\tau+i\beta)} q_i e^{-iH_F\tau}) = \lambda^2 \Phi(\tau) \int u_i u_j \exp\left(-\frac{1}{2}\tilde{u}A(\tau)u + B(\tau)u\right) du.$$

where we have defined the index $j = i + N$, N being the number of degrees of freedom of the system. This type of integral can be easily computed using the identity

$$\left(\frac{d^2}{dS_i dS_j}\right)_{S=B} \int \exp\left(-\frac{1}{2}\tilde{u}Au + Su\right) du = \int u_i u_j \exp\left(-\frac{1}{2}\tilde{u}Au + Bu\right) du$$

which gives

$$f(\tau) = f_\circ(\tau) \left[\frac{(A^{-1})_{ij}}{2} + \sum_j (A^{-1})_{ij} B_j\right]$$

Higher order terms could be eventually evaluated using Wick's theorem.[57]

The evaluation of the trace in equation 11 follow the same lines. Indeed we have

$$k(t) = -2\hbar^{-2} V^2 \mathrm{Re} \int_0^t g(t,\tau) d\tau$$

where

$$g(t,\tau) = Z_G^{-1} \mathrm{Tr}(e^{-i(t-\tau)H_A} e^{-\beta H_G} e^{itH_A} e^{-i\tau H_F})$$

which can be explicitely written as

$$g(t,\tau) = Z_G^{-1}\mathrm{Re}\int \rho_A(q,x,i(t-\tau))\rho_G(x,y,\beta)\rho_A(y,z,-it)\rho_F(z,q,i\tau)dqdxdydz.$$

Since the density matrices of states $|G\rangle$ and $|F\rangle$ are represented in the normal coordinates of the state $|A\rangle$ using the transformations

$$q_G = d_G + J_G q_A \qquad q_F = d_F + J_F q_A$$

we can write explicitly all the terms in the exponents obtaining

$$g(t,\tau) = Z_G^{-1}(2\pi)^{-2N}|\det(J_F J_G)|\exp\left(-\tilde{d}_F T_F d_F - \tilde{d}_G T_G d_G\right)$$
$$D_A(i(t-\tau))D_G(\beta)D_A(-it)D_F(i\tau)\int du\exp\left(-\frac{1}{2}\tilde{u}Au + Bu\right)$$

where

$$A = \frac{1}{2}\begin{pmatrix} M_A(i(t-\tau)) + M'_F(i\tau) & S_A(i(t-\tau)) & 0 & S'_F(i\tau) \\ \tilde{S}_A(i(t-\tau)) & M_A(i(t-\tau)) + M'_G(\beta) & S'_G(\beta) & 0 \\ 0 & \tilde{S}'_G(\beta) & M_A(-it) + M'_G(\beta) & S_A(-it) \\ \tilde{S}'_F(i\tau) & 0 & \tilde{S}_A(-it) & M_A(-it) + M'_F(i\tau) \end{pmatrix}$$

and

$$\tilde{B} = -\begin{pmatrix} \tilde{J}_F T_F(i\tau) J_F \Delta_F \\ \tilde{J}_G T_G(\beta) J_G \Delta_G \\ \tilde{J}_G T_G(\beta) J_G \Delta_G \\ \tilde{J}_F T_F(i\tau) J_F \Delta_F \end{pmatrix}$$

the definitions of the functions $D_X(\lambda), M_X(\lambda), S_X(\lambda)$ have been given previously. Then, after

performing the multidimensional Gaussian integral, one obtain the expression

$$g(t,\tau) = Z_G^{-1} |\det(J_F J_G)| \exp\left(-\tilde{d}_F T_F d_F - \tilde{d}_G T_G d_G\right) \\ D_A(i(t-\tau)) D_G(\beta) D_A(-it) D_F(i\tau) \det(A)^{-1/2} \exp\left(\frac{1}{2}\tilde{B} A^{-1} B\right). \quad (21)$$

Acknowledgement

We acknowledge the financial support by the ImPACT project (FIRB 2012, RBF12CLQD-002) from Ministero dell'Istruzione, dell'Università e della Ricerca. The CINECA award HP10CJUOAA under the ISCRA initiative, for the availability of high performance computing resources and support is also acknowledged.

References

(1) Domcke, W.; Stock, G. Theory of ultrafast nonadiabatic excited-state processes and their spectroscopic detection in real time. In *Adv. Chem. Phys.*; 1997; Vol. 100, p 1.

(2) Zewail, A. H. *The Chemical Bond: Structure and Dynamics*; Academic Press, 1992.

(3) Strümpfer, J.; Schulten, K. *J. Chem. Theor. Comput.* **2012**, *8*, 2808–2816.

(4) Tanimura, Y.; Kubo, R. *J. Phys. Soc. Jpn.* **1989**, *58*, 1199–1206.

(5) Wang, H.; Thoss, M. *J. Chem. Phys.* **2003**, *119*, 1289–1299.

(6) Luo, B.; Ye, J.; Guan, C.; Zhao, Y. *Physical Chemistry Chemical Physics* **2010**, *12*, 15073–15084.

(7) Lax, M. *J. Chem. Phys.* **1952**, *20*, 1752–1760.

(8) Kubo, R. *Phys. Rev.* **1952**, *86*, 929.

(9) Kubo, R.; Toyozawa, Y. *Prog. Theor. Phys.* **1955**, *13*, 160–182.

(10) Peng, Q.; Yi, Y.; Shuai, Z.; Shao, J. *J. Chem. Phys.* **2007**, *126*, 114302–8.

(11) Borrelli, R.; Peluso, A. *Phys. Chem. Chem. Phys.* **2011**, *13*, 4420–4426.

(12) Niu, Y.; Peng, Q.; Deng, C.; Gao, X.; Shuai, Z. *J. Phys. Chem. A* **2010**, *114*, 7817–7831.

(13) Woywood, C.; Domcke, W.; Sobolewski, A. L.; Werner, H.-J. *J. Chem. Phys.* **1994**, *100*, 1400.

(14) Borrelli, R.; Peluso, A. *J. Chem. Phys.* **2003**, *119*, 8437–8448.

(15) Borrelli, R.; Capobianco, A.; Peluso, A. *Chem. Phys.* **2014**, *440*, 25–30.

(16) Mukamel, S. *Principles of Nonlinear Optical Spectroscopy*; Oxford University Press, USA, 1995.

(17) Breuer, H.-P.; Petruccione, F. *The Theory of Open Quantum Systems*; Oxford University Press, USA, 2002.

(18) Kubo, R. *J. Math. Phys.* **1963**, *4*, 174–183.

(19) Kubo, R. *J. Phys. Soc. Jpn.* **1962**, *17*, 1100.

(20) Van Kampen, N. G. *Physica* **1974**, *74*, 215–238.

(21) Nitzan, A.; Jortner, J. *J. Chem. Phys.* **1973**, *58*, 2412–2434.

(22) Takahashi, K.; Yokota, M. *Mol. Phys.* **1971**, *20*, 663–671.

(23) Izmaylov, A. F.; Mendive–Tapia, D.; Bearpark, M. J.; Robb, M. A.; Tully, J. C.; Frisch, M. J. *J. Chem. Phys.* **2011**, *135*, 234106–234106–14.

(24) Jang, S.; Jung, Y.; Silbey, R. J. *Chem. Phys.* **2002**, *275*, 319–332.

(25) Coalson, R. D.; Evans, D. G.; Nitzan, A. *J. Chem. Phys.* **1994**, *101*, 436–448.

(26) Cho, M.; Silbey, R. J. *J. Chem. Phys.* **1995**, *103*, 595–606.

(27) Parson, W. W.; Warshel, A. *J. Phys. Chem. B* **2004**, *108*, 10474–10483.

(28) Pisliakov, A. V.; Gelin, M. F.; Domcke, W. *J. Phys. Chem. A* **2003**, *107*, 2657–2666.

(29) Sharp, T. E.; Rosenstock, K. M. *J. Chem. Phys.* **1964**, *41*, 3453–3463.

(30) Borrelli, R.; Capobianco, A.; Peluso, A. *Can. J. Chem.* **2013**, *91*, 495–504.

(31) Huh, J.; Berger, R. *Faraday Discuss.* **2011**, *150*, 363–373.

(32) Borrelli, R.; Di Donato, M.; Peluso, A. *Biophys. J.* **2005**, *89*, 830–841.

(33) Capobianco, A.; Borrelli, R.; Noce, C.; Peluso, A. *Theor. Chem. Acc.* **2012**, *131*, 1181.

(34) Ferrer, F. J. A.; Santoro, F. *Phys. Chem. Chem. Phys.* **2012**, *14*, 13549–13563.

(35) Freed, K. F. *J. Phys. Chem. B* **2003**, *107*, 10341–10343.

(36) Mebel, A. M.; Hayashi, M.; Liang, K. K.; Lin, S. H. *J. Phys. Chem. A* **1999**, *103*, 10674–10690.

(37) Tang, J.; Lee, M. T.; Lin, S. H. *J. Chem. Phys.* **2003**, *119*, 7188–7196.

(38) Tang, J. *Chem. Phys.* **1994**, *188*, 143–160.

(39) Borrelli, R.; Thoss, M.; Wang, H.; Domcke, W. *Mol. Phys.* **2012**, *110*, 751–763.

(40) Freed, K. F.; Jortner, J. *J. Chem. Phys.* **1970**, *52*, 6272–6291.

(41) Borrelli, R.; Peluso, A. *Wiley Interdisciplinary Reviews: Computational Molecular Science* **2013**, *3*, 542–559.

(42) Domcke, W.; Yarkony, D. R. *Ann. Rev. Phys. Chem* **2012**, *63*, 325–352.

(43) Grebenshchikov, S. Y.; Borrelli, R. *J. Phys. Chem. Lett.* **2012**, *3*, 3223–3227.

(44) Fox, R. F. *J. Math. Phys.* **1975**, *16*, 289–297.

(45) Husimi, K. *Proceedings of the Physico-Mathematical Society of Japan. 3rd Series* **1940**, *22*, 264–314.

(46) Borrelli, R.; DiDonato, M.; Peluso, A. *J. Chem. Theor. Comput.* **2007**, *3*, 673–680.

(47) Wiberg, K. B. *J. Comput. Chem.* **2004**, *25*, 1342–1346.

(48) Borrelli, R.; Peluso, A. *J. Chem. Phys.* **2006**, *125*, 194308–194315.

(49) Borrelli, R.; Peluso, A. *J. Chem. Phys.* **2013**, *139*, 159902.

(50) Borrelli, R.; Capobianco, A.; Peluso, A. *Can. J. Chem.* **2013**, *91*, 495–504.

(51) Peluso, A.; Borrelli, R.; Capobianco, A. *J. Phys. Chem. A* **2009**, *113*, 14831–14837.

(52) Reimers, J. R. *J. Chem. Phys.* **2001**, *115*, 9103–9109.

(53) Martin, J. L.; Breton, J.; Hoff, A. J.; Migus, A.; Antonetti, A. A. *Proc. Natl. Acad. Sci. USA* **1986**, *83*, 957.

(54) Arlt, T.; Schmidt, S.; Kaiser, W.; Lauterwasser, C.; Meyer, M.; Scheer, H.; Zinth, W. *Proc. Natl. Acad. Sci. USA* **1993**, *90*, 11757–11761.

(55) Lauterwasser, C.; Finkele, U.; Scheer, H.; Zinth, W. *Chem. Phys. Lett.* **1991**, *183*, 471–477.

(56) Parson, W. W.; Warshel, A. *Chem. Phys.* **2004**, *296*, 201–216.

(57) Wick, G. C. *Phys. Rev.* **1950**, *80*, 268–272.

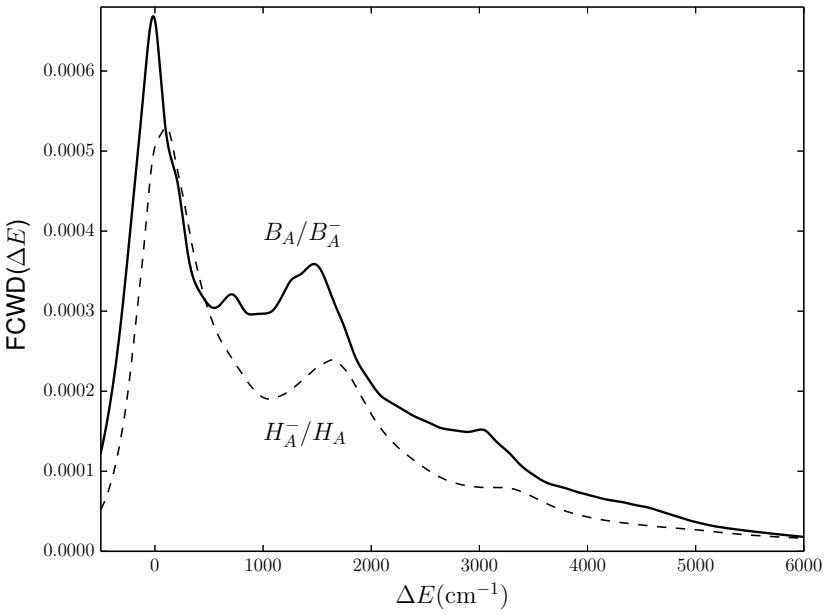

Figure 1: Franck-Condon weighted density of states for the electron detachment process $\mathrm{BChl}^- \rightarrow \mathrm{BChl} + e^-$, full line, and for the electron injection process $\mathrm{H_A} + e^- \rightarrow \mathrm{H_A}^-$, dashed line, at $T = 298K$.

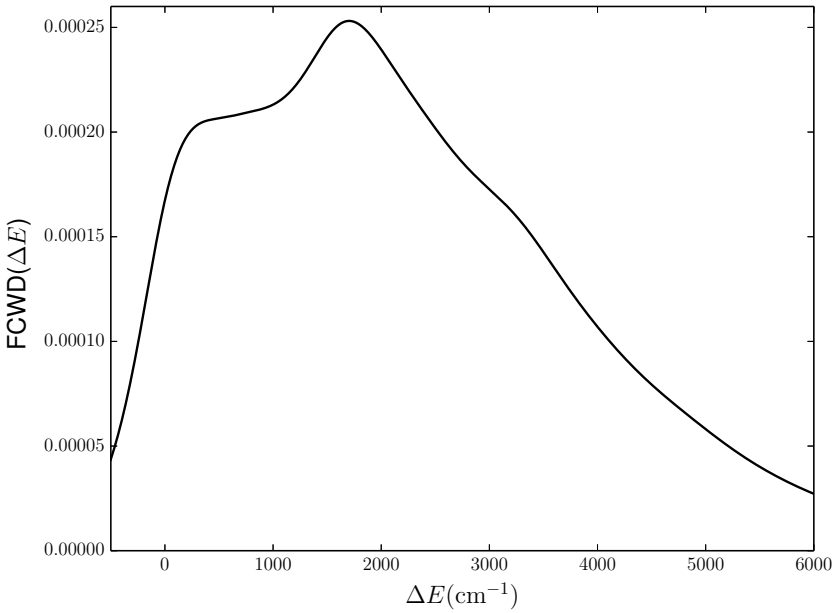

Figure 2: Franck-Condon weighted density of states for the electron transfer process $\mathrm{B_A^-} + \mathrm{H_A} \rightarrow \mathrm{B_A} + \mathrm{H_A}^-$, at $T = 298K$.

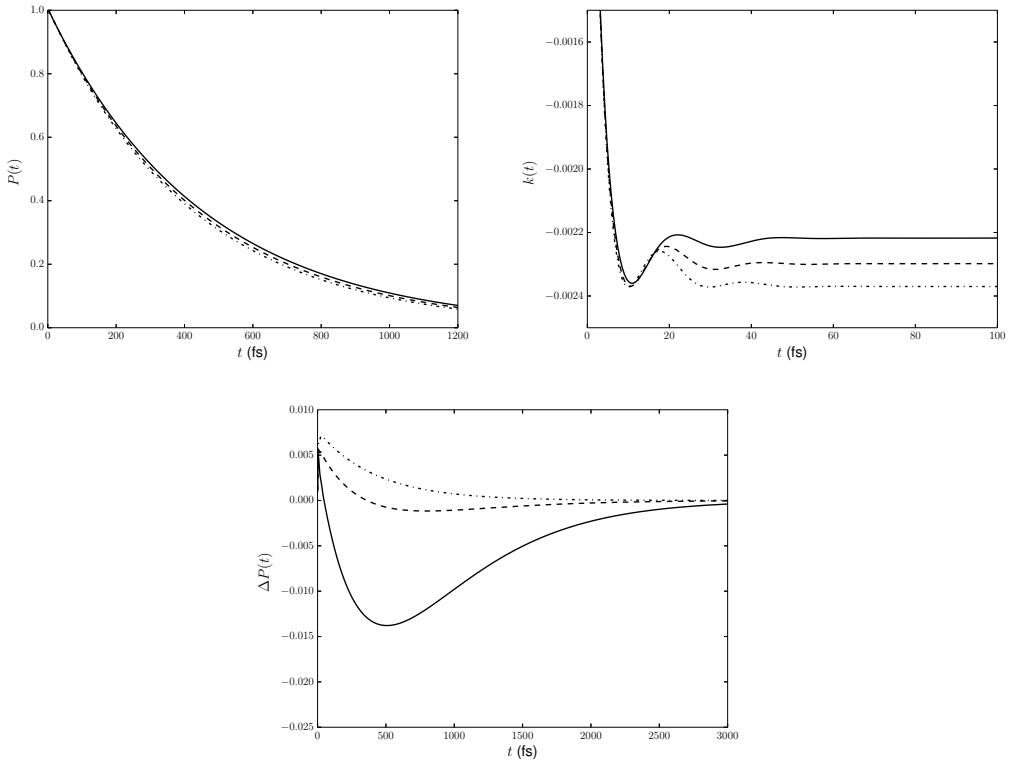

Figure 3: a) Population of the electronic state $\left|B_A^-/H_A\right\rangle$ as a function of time. The system is initially found in a thermally equilibrated distribution. b) ET rate $k(t)$ as a function of time. c) Difference between the population of the initial electronic state and the exponential decay of the standard FGR approach. The curves represent the result for different values of ΔE_{AF}. Full line $\Delta E_{AF} = 1250$ cm^{-1}; dashed line $\Delta E_{AF} = 1350$ cm^{-1}; dotted line $\Delta E_{AF} = 1450$ cm^{-1}.

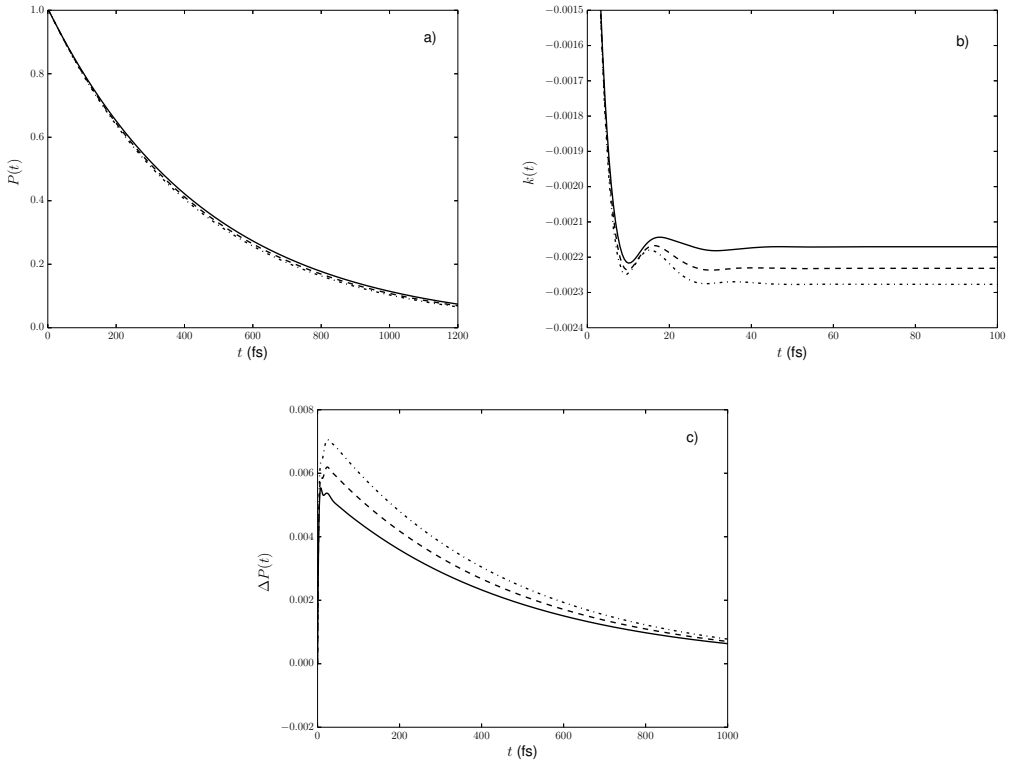

Figure 4: a) Population of the electronic state $\left|B_A^-/H_A\right\rangle$ as a function of time. The system is initially found in a non-equilibrium distribution (see text). b) ET rate $k(t)$ as a function of time. c) Difference between the population of the initial electronic state and the exponential decay of the standard FGR approach. The curves represent the result for different values of ΔE_{AF}. Full line $\Delta E_{AF} = 1250$ cm^{-1}; dashed line $\Delta E_{AF} = 1350$ cm^{-1}; dotted line $\Delta E_{AF} = 1450$ cm^{-1}.